



ISSN (E): 2277-7695

ISSN (P): 2349-8242

NAAS Rating: 5.23

TPI 2022; 11(10): 01-08

© 2022 TPI

www.thepharmajournal.com

Received: 09-07-2022

Accepted: 17-09-2022

Putta Aparna

Department of Textile and Apparel Designing, College of Community Science, University of Agricultural Sciences, Dharwad, Karnataka, India

Dr. Jyoti V Vastrad

Department of Textile and Apparel Designing, College of Community Science, University of Agricultural Sciences, Dharwad, Karnataka, India

Green waste mediated Zinc Oxide nanoparticles with citrus peel

Putta Aparna and Dr. Jyoti V Vastrad

Abstract

The synthesis of metal oxide nanoparticles with the use of plant extracts is a promising alternative to the conventional chemical method. This study aims to synthesize green zinc oxide nanoparticles with zinc acetate dihydrate precursor using *Citrus reticulata* peel powder. The synthesized nanoparticles were characterized for different analytic techniques. The maximum UV-Vis absorption peak was observed at 357 nm wavelengths which is specific for zinc oxide nanoparticles with a greater particle size of 36 nm. The FT-IR result shows a strongest absorption bands at 651 cm^{-1} , which resulted from a covalent bond between zinc metal and oxygen atoms (Zn-O). According to SEM analysis, the morphology of the biosynthesized ZnO NPs were predominantly spherical in shape. Furthermore, the purity of the ZnO NPs was also confirmed by ED's analysis. The crystallinity of the biosynthesized ZnO NPs was confirmed by XRD analysis, revealing sharp and narrow diffraction peaks, confirming the hexagonal wurtzite structure of the ZnO NPs.

Keywords: green synthesis, citrus reticulate, zinc oxide nanoparticles (zno nps), extract, precursor

1. Introduction

Metal nanoparticles synthesis is a fascinating subject in nano science. Several research groups have been interested in various forms of metal NPs, including as iron oxide, silver nitrate, copper oxide and zinc oxide, in the previous few decades. Metal oxides such as TiO_2 , ZnO, MgO, and CaO are of particular importance among inorganic materials since they are not only stable under extreme conditions, but are also usually recognized as safe materials for humans and animals. Among this Zinc oxide (ZnO) nanomaterials have remarkable potential for applications in many different areas such as solar cells, sensors, piezoelectric devices, photodiode devices, sunscreens, and anti-reflection coatings and photo catalysis (Sharma *et al.*, 2020). It also exhibits effects by inducing ROS generation and causing apoptosis. ZnO NPs shows synergistic and enhanced therapeutic efficacy when combined with other therapeutic agents. ZnO nanoparticles have also been explored as drug carriers for anti-cancer drugs. Zinc oxide is a modifier in the textile industry because of its use for the production of safety garments and all kinds of fabric for technical applications (Mishra *et al.*, 2017) ^[6].

Metal nanoparticles are synthesized using different approaches, including the sol-gel method, thermal decomposition, hydrothermal and microwave irradiation and many more. However, due to the formation of a large number of secondary waste products as a result of the incorporation of chemical agents for the reduction process, these chemical and physical synthesis procedures are time-consuming, costly, and toxic (Gupta *et al.*, 2018) ^[10]. Metal nanoparticles synthesized from plants and/or plant extracts are more stable than those produced by other organisms. Modified organisms have a strong ability to optimize the synthesis of additional proteins, enzymes, and biomolecules that are required for nanoparticle production and stability. Thus *citrus reticulata* peel was selected as a catalyst for synthesis of green zinc oxide nanoparticles. Citrus fruits are commonly used in food processing industries, where tons of pulp peel and rags are thrown solid waste during the extraction process. The fruit waste generation not only results in financial losses but also adds to the expense of waste management and disposal. Thus to minimize the fruit wastage and protect the environment, an experimental study was conducted by using *citrus reticulata* peel as a catalyst in the green synthesis of zinc oxide nanoparticles different solvent extracts.

2. Materials and Methods**2.1 Selection and preparation process of *Citrus reticulata* peel powder**

Nagpur orange is a variety of mandarin orange (*Citrus reticulata*) grown in Nagpur, Maharashtra, India. The fruit has a pockmarked exterior and sweet and juicy pulp. It gives the city of Nagpur its pseudonym Orange City.

Corresponding Author:**Putta Aparna**

Department of Textile and Apparel Designing, College of Community Science, University of Agricultural Sciences, Dharwad, Karnataka, India

The Nagpur oranges blossom during the Monsoon season and are ready to be harvested from the month of December. The orange crop here grows twice a year. The fruit is available from September to December, which has a slightly sour taste. It is followed by the sweeter Mrig crop in January (en.wikipedia.org/wiki/Nagpur_orange).

For the study Orange fruits of the Nagpur variety were collected from the local market of Dharwad. Collected fruits were cleaned thoroughly using distilled water the peel and their edible portions were separated. The peels were oven-dried at 35 °C for 48 h, pulverized and sieved with ASTM standard mesh and stored in an air container for further experiment (Mahmoud *et al.*, 2016) [5]. The details of the extraction procedure were represented in Plate 1.

Table 1: Yield of the *Citrus reticulata* peel extract

Weight of fruits	Wet weight (gm)	Dry weight (gm)	Yield of powder after sieving (gm)
1 kg	135.4	81.4	43.4

2.2 Extraction procedure

2.2.1 Aqueous extraction

For aqueous extraction, 100 ml of Milli Q water was taken in the beaker and heated until the temperature rises to 100 °C with a magnetic stirrer and then 2 grams of *Citrus reticulata* peel powder was added to the beaker and kept for stirring at 100 °C for 20 minutes. After cooling to room temperature, the extract was filtered through Whatman paper no.1 and stored in the refrigerator for further use.

2.3 Green synthesis of Zinc Oxide nanoparticles

Zinc acetate dihydrate precursor was selected as a precursor for the study and *Citrus reticulata* powder as a catalyst for the green synthesis of zinc oxide nanoparticles. For nanoparticles production, zinc acetate dihydrate precursor was dissolved in Milli-Q water and stirred for four to five hours by adding *C. reticulata* peel extract. Sodium hydroxide was added drop by drop to maintain the pH of the solution (Chitha *et al.*, 2015) [4]

2.4 Characterization of green zinc oxide nanoparticles

The characterization of green synthesized zinc oxide nanoparticles was carried out for different parameters such as absorbance peak by UV-Visible spectrophotometer, particle size, morphology by Scanning Electron Microscope (SEM) with EDS, functional groups with FTIR and structure with XRD. The optimized treatment concentrations obtained during the study were taken for further characterization using following instruments.

2.4.1 UV-Visible spectrophotometer

The absorbance peak of synthesized and standard ZnO NPs was measured using a UV-Visible spectrophotometer. It works on the principle of Beer-Lambert's law. This law states that, the greater the number of absorbing molecules (that have the ability to absorb light of a specific wavelength), the greater the extent of absorption of the radiation.

$$A = \log (I_0/I) = ECL \quad (1)$$

Where,

A = Absorbance

I_0 = Intensity of light upon sample cell (cd)

I = Intensity of light departing from sample cell (cd)

E = Molar absorptivity (L/mol. m)

C = Concentration of solute (mol/L)

L = Length of sample cell (m)

From the Beer-Lambert law, it is determined that the greater the number of molecules that are capable of absorbing light at a certain wavelength, the greater is the extent of the absorption of light. An optical spectrophotometer records the wavelengths at which absorption occurs, together with the degree of absorption at each wavelength. The wavelength that corresponds to the highest absorption is usually referred to as λ_{max} . The resulting spectrum was presented as a graph of absorbance (A) versus wavelength (λ). For ZnO NPs, the absorbance peak (λ_{max}) ranges from 300 to 400 nm (Santhoshkumar *et al.* 2017) [16].

The sample was prepared by diluting 1 mL of ZnO NPs into 2 mL of distilled water and measuring the UV-Visible spectrum of solutions (UV probe Version 2.61) (Habibi *et al.*, 2017) [13].

Table 2: The parameters used while testing UV-Visible spectrophotometer are as follows:

Wavelength range (nm)	300 to 400
Scan speed	Medium
Sampling interval	0.20
Auto sampling interval	Enabled
Scan mode	Auto

2.4.2 Particle size Analyzer

The particle size of synthesized ZnO NPs was measured using PSA. The zeta sizer (nano series) performs size measurements using a process called Dynamic Light Scattering (DLS). The principle of DLS is that fine particles and molecules are in constant random thermal motion, called Brownian motion, which diffuses at a speed related to their size. Smaller particles diffuse faster than larger particles. The speed of Brownian motion is also determined by the temperature, therefore precision temperature control is essential for accurate size measurement. The particle measurement can be observed from 0.6 nm to 8.9 μ m. The synthesized ZnO nanoparticle samples were subjected to sonication to obtain a homogenous population of ZnO nanoparticles. Then samples were analyzed through a particle size analyzer (Nicomp, NANOZ Z3000 PSS) to determine the mean size and % distribution (Ahmed *et al.*, 2018) [16].

2.4.3 Fourier transform infrared spectroscopy (FT-IR) study

The presence of functional groups in biomolecules of orange peel extract used for the phytosynthesis of zinc oxide nanoparticles was studied by an FT-IR spectrometer (Shimadzu, IR-Tracer100) with the Attenuated Total Reflectance (ATR) technique. The unique advantage of ATR-FTIR imaging is that it requires minimal or no sample preparation before spectral measurements because the penetration depth of IR light in the sample for ATR measurements is independent of sample thickness. In brief, 1 to 2 drops of ZnO nanoparticle samples were placed on the ATR sample loader and analysed to obtain a good signal-to-noise ratio. 25 scans of ZnO nanoparticles were taken in the range of 4000-400 cm^{-1} and the resolution was kept at 4 cm^{-1} .

2.4.5 Surface morphology using Scanning Electron Microscope (SEM)

The surface morphology of synthesized ZnO NPs was measured using a Scanning Electron Microscope (SEM). SEM is a powerful magnification tool that utilizes focused beams of electrons to obtain information. It works on the principle that when accelerated primary electrons strike the sample in a vacuum chamber, it produces secondary electrons. These secondary electrons are collected by a positively charged electron detector, which in turn gives a 3D image of the sample using the software (Smart SEM, Version V05.05) and backscattered electrons are higher energy electrons that are elastically backscattered by the atoms of the sample.

Atoms with higher atomic numbers backscatter more efficiently, and therefore this detector can give compositional information about the sample (Haq *et al.*, 2014) [12]. Resolution in a perfect optical system can be described mathematically by Abbe's equation, as given in the equation

$$d = 0.612 \lambda / n \sin \alpha \quad (2)$$

Where,

d = Resolution (nm)

λ = Wavelength (nm)

n = Refractive index

α = Aperture angle (deg)

The aluminium stub (1cm dia.) was cleaned to remove surface oils or dirt by using isopropyl alcohol and blowing with compressed air. It was then placed on the sample holder. The double-coated conductive carbon tape was used as an adhesive and pasted on the stub. The thin layer of a dried sample of 0.2 g was dropped on the adhesive surface uniformly and again blown with compressed air and then coated with gold-palladium to make the samples conductive using a sputter coater for about 90 s (Quorum Technologies, OM-SC7620, London, United Kingdom). The sample holder was removed from the sputter coater and placed in the vacuum chamber. The magnification (1 to 500 kX) and focusing were carried out to get a clear surface morphology of samples at the accelerating voltage range of 1 to 30 kV with the working distance of the sample at 10 mm (8 to 25 mm) (Kim *et al.*, 2009) [14].

2.4.6 Phase identification by X-Ray Diffractometer (XRD)

Phase identification of synthesized ZnO NPs was measured using an X-Ray Diffractometer (XRD): XRD is a unique method for determining the crystallinity of a compound. It is based on the constructive interference of monochromatic X-Rays and a crystalline sample. The X-rays are generated by a cathode ray tube filtered to produce monochromatic radiation and directed towards the sample. The interaction of the incident rays with the sample produces constructive interference when conditions satisfy Bragg's law (Halawani, 2017). Inter-planar spacing between atoms (d-spacing) was calculated by using Bragg's Law (1912) as given below in the equation

$$d = \frac{n\lambda}{2\sin\theta} \quad (3)$$

Where,

λ = Wave length of X-Ray (0.1540 nm)

θ = Diffraction angle (deg)

n = Integer called order of diffraction

Crystalline nature of the ZnO NPs was measured on X-Ray diffractometer operated at voltage (20 to 60 kV) and current (2 to 60 mA). Spectrum was recorded by $\text{CuK}\alpha$ radiation with wavelength of 1.5406 Å in the 2θ range of 20 to 80°. Synthesized ZnO NPs of (1 g) were uniformly spread on glass sample holder and placed in scanning chamber. The scan speed and step size were set by using ICDD PDF₂ software (Version V6.7) of 0.30 °/min and 0.001 s, respectively and were fixed (Djangan *et al.*, 2015) [7]. The XRD pattern was recorded for phase identification of ZnO NPs.

3. Results and Discussion

3.1 Visual analysis of ZnO NPs formation

Adding *Citrus reticulata* peel powder to zinc acetate dihydrate leads to physio-chemical changes in the aqueous solution. The most apparent of these is a change in the colour of the reaction mixture after 2 hours, which is regarded as an early marker for the formation of NPs these is a change in the colour of the reaction mixture after 2 hours, which is regarded as an early marker for the formation of NPs. A change in hue from pale yellow to dark yellowish mud brown was observed in nanoparticles indicating the formation of ZnO NPs in at 4% concentration. The transformation of zinc ions to ZnO NPs is hypothesized to be mediated by flavonoids and phenolic substances. The colour of the solution stopped changing after a few hours, indicating that the ZnO salt had been completely bio-reduced into nanoparticles. Plate 1 and 1 depict the change in colour of the reaction mixtures as a result of the formation of ZnO NPs.

3.2 UV-Visible spectroscopy of green zinc oxide nanoparticles

The optical properties of synthesized ZnO NPs were characterized based on UV absorption spectra with a wavelength range between 300 nm and 400 nm, Jayachandran and Umar (2021). The majority of the nanoparticles did not have an absorption peak at a specific wave length. The nanoparticles synthesised with at 90 °C with 4 a % concentration of *Citrus reticulata* peel powder showed a peak at 362.5 nm, with a better particle size distribution and represented in Fig 1. The absorption peak for zinc oxide is prominent in the wavelength range (360–362.5 nm) due to band-gap absorption, which occurs when electrons are removed from the valence band and transferred to the conduction band. In addition, as ZnO particles are nano-scale and the particle size distribution is limited, a strong absorption peak appears at (200-400) nm.

3.3 Particle size analyzer (PSA)

The size of the green synthesized zinc oxide nanoparticles were analyzed using particle size analyzer (PSA) in terms of mean diameter, % size distribution with the intensity-weight, number-weight and volume-weight of the nanoparticles. The nanoparticles produced at 4% concentration of zinc acetate precursor had an average particle size of 33.6 nm, as shown in Fig. 2. The reduction in particle size may be due to several factors, such as pH of the reaction mixture, reaction time, stirring speed, nature of capping agents, and concentration of metal precursors, which greatly affect the properties of the zinc oxide nanoparticles and their applications (Shaba *et al.*, 2021) [17].

3.4 Fourier transform infrared spectrometer analysis

An FT-IR study was carried out to identify the functional groups responsible for the reduction of ZnO nanoparticles and to identify the biomolecules involved in the reduction and capping of bio-reduced zinc oxide nanoparticles with *Citrus reticulata* peel powder. The analysis was performed in a frequency range of 4500-500 cm^{-1} , at room temperature. Fig 3 represents the functional groups of green ZnO NPs produced with the ZnO-1 precursor. It is observed that different peaks were obtained at 651, 948, 1014, 1562 and 2937 cm^{-1} . FTIR spectra also exhibited a broad peak at around 3263 and 3726 cm^{-1} in a higher energy region due to O-H stretching of alcohols and phenols. Absorption bands at 1562 cm^{-1} are due to the C-C stretching aromatic ring, 2937 represents -CH stretch and 1014 cm^{-1} C-O stretching of esters and carboxylic functional. The strongest absorption bands were observed at 651 cm^{-1} , which resulted from a covalent bond between zinc metal and oxygen atoms (Zn-O). The FTIR spectrum reveals that *C. reticulata* peel extract contains a substantial amount of diverse chemical groups such as -OH, COOH, and amine. Furthermore, there is a hydroxyl group due to the presence of phenols. Polyphenolic tannins prevent aggregation and aid in the reduction and stabilization of ZnO nanoparticles. So, the physicochemical properties of *Citrus reticulata* peel powder act as a bio template to stop the particles from sticking together.

3.5 Scanning electron microscopy and EDX analysis

Performing a visual analysis of a surface using scanning electron microscopy contributes to the identification of contaminants or unknown particles. SEM analysis is used for morphological information and particle characterization. The SEM images were seen at different magnification ranges from

2 μm -200 nm. Nanoparticles synthesized were spherical in shape, with an average diameter range of 33.6 to 120 nm, as shown in Fig 4(a). The existence of metallic zinc oxide in green synthesized ZnO NPs was confirmed by EDX data, as shown in Fig. 4(b). Zinc (29.81%), oxygen (43.56%) and carbon (26.64%) were the elemental compositions determined by EDX analysis. It is clear that the precursors have played a vital role in the surface morphology and structure of ZnO NPs. Demissie *et al.* (2020) used SEM and TEM to analyze biosynthesized ZnO NPs made with "Lippia adoensis" and found that they had a spherical shape and nanorod-shaped structures.

Noorjahan (2019)^[15], with Keezhanelli (*P. niruri*) leaf extract, showed a colour change from pale white to brown and a cylindrical morphology with an average size of 5 nm with SEM analysis.

3.6 X-ray diffraction (XRD) analysis

X-ray diffraction analysis (XRD) is a technique used in materials science to determine the crystallographic structure of a material. The XRD spectrum of the synthesized ZnO nanoparticles with ZnO-1 precursor is shown in Fig.5. The intense diffraction peaks are 69.42°. These peaks corresponding to the diffraction planes of (100), (002), (101), (102), (110), (103) and (112) agree well with the JCPDS Card No. 36-1451. As shown, the position and intensity of the diffraction peaks match between them, confirming the hexagonal wurtzite structure of the ZnO NPs. This fact confirms that the synthesized ZnO NPs are in a hexagonal wurtzite structure. Furthermore, no other distinctive peaks occur besides the ZnO, indicating the sample's with high purity. These findings are backed up by research (Gnanasangeetha and Thambavani, 2014)^[9]



Plate 1: Colour change of zinc oxide nanoparticles

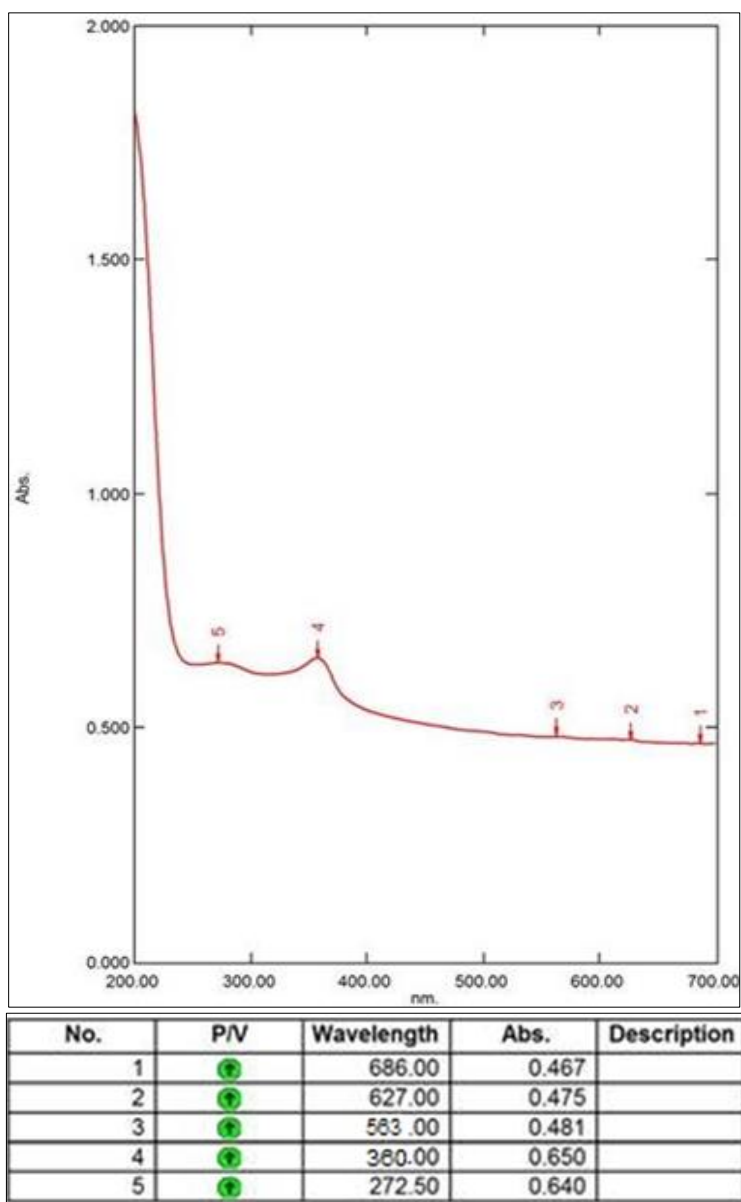


Fig 1: Absorption peaks of green zinc oxide nanoparticle

Mean Diam	= 33.6 nm	Variance (P.I.)	= 0.069
Std. D	= 8.8 nm (26.3%)	Chi Squared	= 2.236

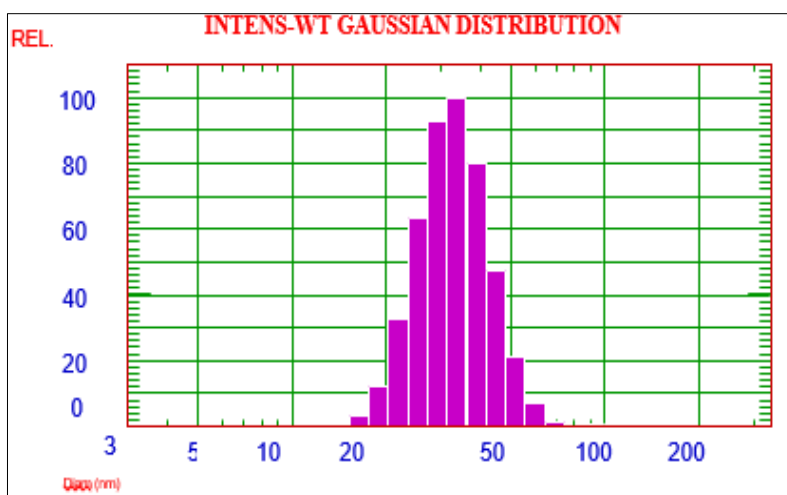
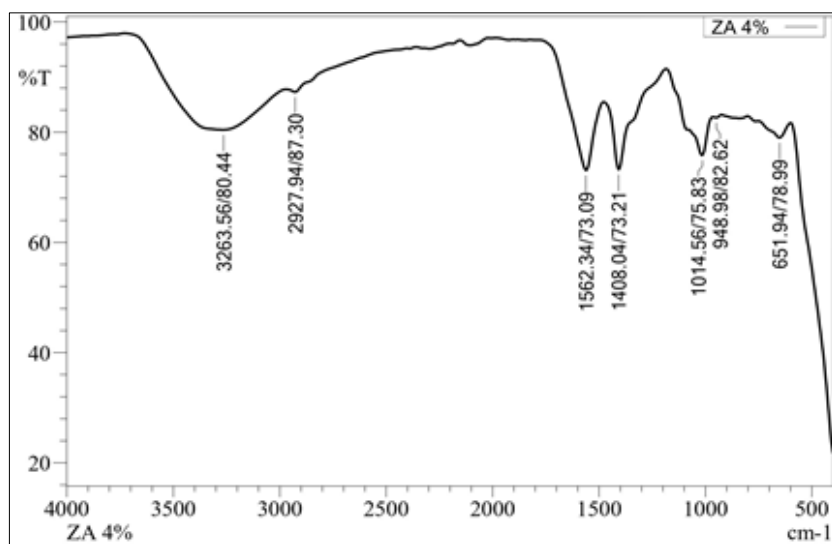


Fig 2: Particle size distribution of green zinc oxide nanoparticles



	Peak	Intensity	Corr. Intensity	Base (H)	Base (L)
1	651.94	78.99	2.82	752.24	601.79
2	948.98	82.62	0.30	964.41	925.83
3	1014.56	75.83	5.93	1080.14	964.41
4	1408.04	73.21	13.69	1477.47	1184.29
5	1562.34	73.09	15.56	1778.37	1477.47
6	2927.94	87.30	1.03	2970.38	2403.30
7	3263.56	80.44	11.28	3726.47	2970.38

Fig 3: Fourier transform infrared spectrometer analysis of green zinc oxide nanoparticles

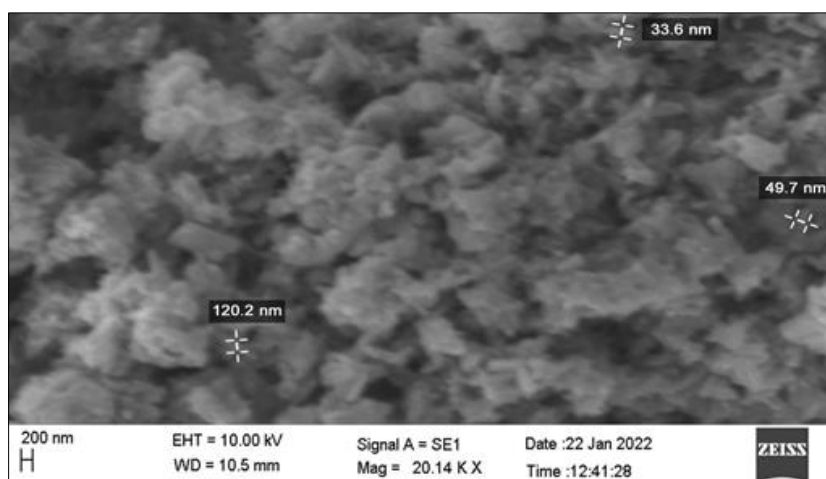


Fig 4(a): Scanning electron microscopy of green ZnO NPs

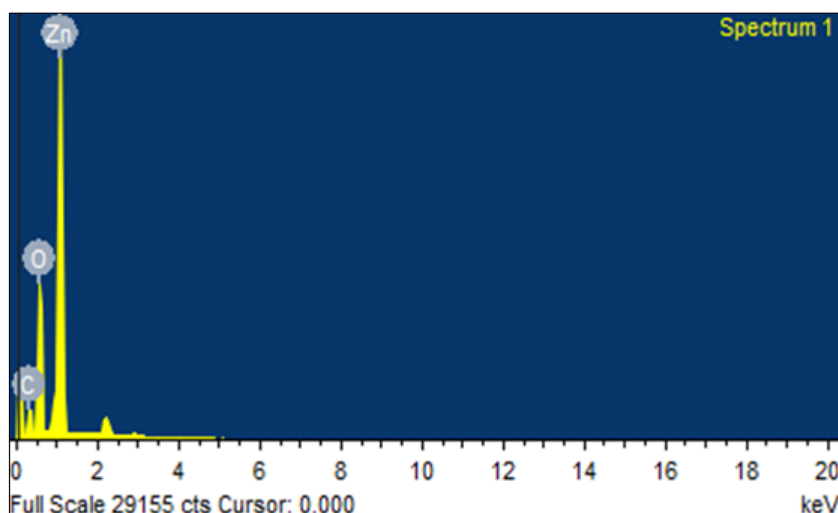


Fig 4(b): Energy dispersive X-ray analysis of green ZnO NPs

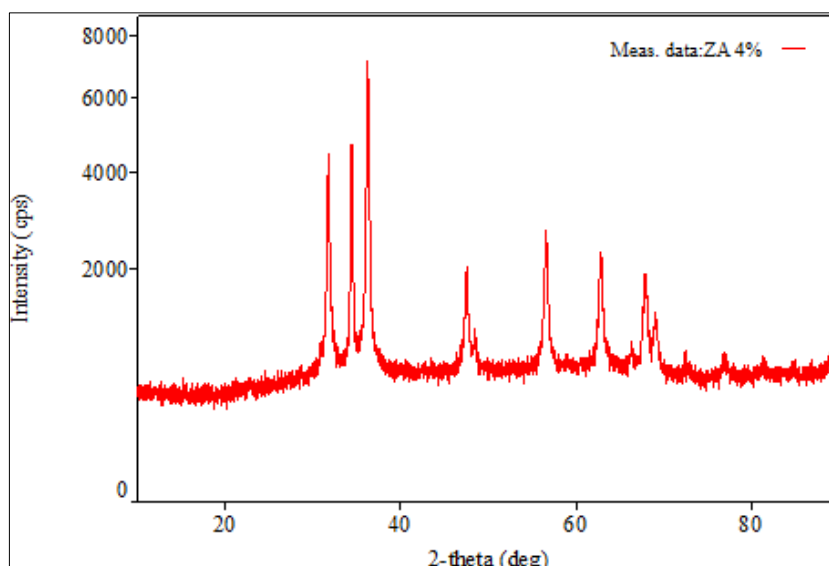


Fig 5: XRD analysis of green zinc oxide nanoparticles

4. Conclusion

Using a green synthesis to produce ZnO NPs by using *Citrus reticulata* peel powder is achievable. In addition, the study indicates that, these substrate functions as reducing and stabilizing compound for synthesis of zinc oxide nanoparticles with zinc acetate dehydrate precursor. This environmentally friendly synthesis technique lowers the requirement for harmful compounds by utilizing natural resources. Therefore, the rapidly advancing understanding of green synthesis outlined herein indicates that zinc oxide nanoparticles have immense potential for the development of multifunctional finishing of textiles in the near future using biological extracts.

5. References

- Ahmed KS, Itino T, Ichikawa T. Duration of developmental stages of *Callosobruchus chinensis* (Coleoptera: Bruchidae) on Adzuki bean and the effects of neem and sesame oils at different stages of their development. *Pak. J Biol. Sci.* 2003;6(10):932-335.
- Barzinjy AA, Azeez HH. Green synthesis and characterization of zinc oxide nanoparticles using *Eucalyptus globulus* Labill. Leaf extract and zinc nitrate hexahydrate salt. *SN Appl. Sci.* 2020;2(5):36-39.
- Belay A, Mekuria M, Adam G. Incorporation of zinc oxide nanoparticles in cotton textiles for ultraviolet light protection and antibacterial activities. *Nanomater. Nanotechnol.* 2020;10:1-8.
- Chitha MJ, Sathya M, Pushpanathan K. Effect of pH on crystal size and photoluminescence property of ZnO NPs prepared by chemical precipitation method. *Acta Metall Sin (Engl. Lett.)*. 2015;28(3):394-404.
- Mahmoud KF, Ibrahim MA, Mervat ED, Shaaban HA, Kamil MM, Hegazy NA. Nano-encapsulation efficiency of lemon and orange peels extracts on cake shelf life. *American J Food Tech.* 2016;11(3):63-75.
- Mishra PK, Mishra H, Ekielski A, Talegaonkar S, Vaidya B. Zinc oxide nanoparticles: A promising nanomaterial for biomedical applications. *Drug Discov. Today.* 2017;22(12):1825-1834.
- Djangang CN, Mlowe S, Njopwouo D, Revaprasadu N. One-step synthesis of silica nanoparticles by thermolysis of rice husk ash using nontoxic chemicals ethanol and polyethylene glycol. *J Appl. Chem.* 2015;4(4):1218-1226.
- Demissie MG, Sabir FK, Edossa GD, Gonfa BA. Synthesis of zinc oxide nanoparticles using leaf extract of *Lippia adoensis* (Koseret) and evaluation of its antibacterial activity. *J Chem.* 2020:1-9.
- Gnanasangeetha D, Thambavani DS. Biogenic production of zinc oxide nanoparticles using *Acalypha Indica*. *J Chem. Biol. Phy. Sci.* 2013;4(1):238-246.
- Gupta R, Xie H. Nanoparticles in daily life: applications, toxicity and regulations. *J Environ. Pathol. Toxicol. Oncol.* 2018;37:209-230.
- Halawani EM. Rapid biosynthesis method and characterization of silver nanoparticles using *Zizyphus Spina Christi* leaf extract and their antibacterial efficacy in therapeutic application. *J Biomater. Nanobiotechnol.* 2017;8(1):22-35.
- Haq IU, Akhtar K, Malik A. Effect of experimental variables on the extraction of silica from the rice husk ash. *J Chem. Soc. Pak.* 2014;36(3):382-387.
- Habibi B, Hadilou H, Mollaer S, Yazdinezhad A. Green synthesis of silver nanoparticles using the aqueous extract of *Prangos ferulaceae* leaves. *Int. J Nano Dimensions.* 2017;8(2):132-141.
- Kim SK, Sohn EY, Lee IJ. Starch properties of native foxtail millet (*Setaria italica* Beauv). *J Crop Sci. Biotechnol.* 2009;12(1):59-62.
- Noorjahan CM. Green synthesis, characterization and antibacterial activity of zinc oxide nanoparticle. *Asian J Pharma. Clinical Res.* c2019, p.106-110.
- Santhoshkumar J, Kumar VS, Rajesh kumar S. Synthesis of zinc oxide nanoparticles using plant leaf extract against urinary tract infection pathogen. *Resour. Efficiency Technol.* 2017;3:459-465.
- Shaba EY, Jacob JO, Tijani JO, Suleiman MAT. A critical review of synthesis parameters affecting the properties of zinc oxide nanoparticle and its application in wastewater treatment. *Appl. Water Sci.* 2021;11(2): 45-49.
- Verbic A, Sala M, Jerman I, Gorjanc M. Novel green in situ synthesis of ZnO nanoparticles on cotton using

- pomegranate peel extract. *Mater.* 2021;14(16):4472.
19. Vinay CH, Goudanavar P, Acharya A, Ahmed MG. and Kumar PS. Development and characterization of orange peel extract based nanoparticles. *Asian J Pharma. Res.* 2018;8(2):71.
 20. Vastrad JV, Goudar G, Byadgi SA, Devi RD, Kotur R. Identification of bio-active components in leaf extracts of Aloe vera, *Ocimum tenuiflorum* (Tulasi) and *Tinospora cordifolia* (Amrutballi). *J Med. Plants Res.* 2015;9(28): 764-770.